ISA Transactions 53 (2014) 1620–1628

Contents lists available at ScienceDirect

ISA Transactions

journal homepage: www.elsevier.com/locate/isatrans

IMC-PID-fractional-order-filter controllers design for integer order systems

Bettayeb Maâmar [a,b], Mansouri Rachid [c,*]

[a] Electrical & Computer Engineering Department, University of Sharjah, United Arab Emirates
[b] Center of Excellence in Intelligent Engineering Systems (CEIES), King Abdulaziz University, Jeddah, Saudi Arabia
[c] L2CSP Laboratory, Mouloud Mammeri University, Tizi Ouzou, Algeria

ARTICLE INFO

Article history:
Received 3 March 2013
Received in revised form
21 August 2013
Accepted 10 May 2014
Available online 20 June 2014
This paper was recommended for publication by Y. Chen

Keywords:
Fractional order controller
PID controllers
Internal model control
Robust control

ABSTRACT

One of the reasons of the great success of standard PID controllers is the presence of simple tuning rules, of the automatic tuning feature and of tables that simplify significantly their design. For the fractional order case, some tuning rules have been proposed in the literature. However, they are not general because they are valid only for some model cases. In this paper, a new approach is investigated. The fractional property is not especially imposed by the controller structure but by the closed loop reference model. The resulting controller is fractional but it has a very interesting structure for its implementation. Indeed, the controller can be decomposed into two transfer functions: an integer transfer function which is generally an integer PID controller and a simple fractional filter.

1. Introduction

The ubiquitous proportional-integral-derivative (PID) controller has continued to be the most widely used process control technique for many decades. Indeed, PID controllers are still widely used in industrial systems despite the significant developments of recent years, in control theory and technology. This is because they perform well for a wide class of processes. Also, they give robust performance for a wide range of operating conditions. Many possible approaches for determining the tuning of the parameters on appropriate PID controllers have been given in the literature in both time and frequency domain. The literature is very abundant in this field; see for example [1,2].

In control system theory, there are four possible combinations of a system and a controller. The first is the traditional integer-order control where both the system to be controlled and the controller are of integer-order. The second case is a fractional-order plant model controlled by an integer-order controller. There are very few studies that refer to this type of combination [3,4]. The third case is a fractional-order plant model controlled by a fractional-order controller (see for example [5,6]). Nevertheless, because the majority of systems are modeled as integer order ones, fractional order control is mainly applied by using fractional controllers for integer order systems. This case is the most popular and the literature is now abundant, as detailed next.

Fractional-order proportional-integral-derivative (FOPID) controllers have received a considerable attention in the last two decades. They provide more flexibility in controller design as compared with standard PID controllers. This is because they have five parameters to select instead of three parameters in the standard PID controllers. However, this flexibility also implies that tuning of the controller can be much more complex.

The concept of FOPID controllers was proposed by Poblubny [7]. He also demonstrated a better performance using this type of controller as compared with PID controller when controlling a fractional order system. A frequency domain approach using FOPID controllers is also studied in [8]. In [9], an optimization method is presented where the parameters of the FOPID are tuned to satisfy predefined design specifications. Ziegler–Nichols tuning rules for FOPID are reported in [10]. In [11,12], a FO-IP (Fractional Order Integral Proportional) controller design using the pole placement method is proposed. There are several other papers published in recent years where the tuning of FOPID was investigated (see for example [13,14] and the references therein for more information). Further research activities are being done to develop new tuning methods and to investigate new applications of FOPID controllers. In [15], the control of heat diffusion systems using FOPID controllers is studied and different tuning methods are applied. Control of an irrigation canal using FOPID controllers

* Corresponding author.
E-mail addresses: maamar@sharjah.ac.ae (B. Maâmar), rachid_mansouri_ummto@yahoo.fr (M. Rachid).

http://dx.doi.org/10.1016/j.isatra.2014.05.007
0019-0578/

is given in [16]. FOPID controller tuned using a particle swarm optimization algorithm is used to control an automatic voltage regulator system [17]. The internal model control based PID (IMC-PID) tuning method was introduced in the last years to design FOPID controllers. This is due to the main characteristic of IMC; simple structure and intuitive design. Nevertheless, very few studies have been published in this area [18–21].

The dynamic model which governs the phenomenon of "fractional robustness" is non-integer order linear differential equation, and the principle of the CRONE suspension, the synthesis method and the performance are developed for this non-integer order model [22,23]. The research work of Oustaloup with his famous CRONE Controllers have really popularized fractional control. In the CRONE principle, the closed loop reference model is ($F(s) = 1/(1+\tau_c s^{\alpha})$). This particular form has very important properties because its phase margin remains constant independently of the value of the system gain. Thus, the closed loop system is robust to process gain variations and the step response exhibits iso-damping property. In this paper, we focus on integer order systems controlled by fractional order controllers, but a new approach will be investigated. The fractional property is not especially imposed by the controller structure but by the closed loop reference model. The controller thus obtained is necessarily fractional, but has a very interesting structure for its implementation. Indeed, the controller can often be decomposed in two parts. An integer PID controller cascaded with a simple fractional order filter being a fractional integrator ($1/s^{\alpha}$) or a first order fractional model ($1/(1+\tau_f s^{\alpha})$). On the other hand, during our investigations, we ensured that the controller design method is simple to implement.

2. Preliminary

2.1. CRONE principle

In his study on the design of feedback amplifiers, Bode [24] suggested an ideal shape of the open-loop transfer function of the form:

$$L(s) = \frac{1}{\tau_c\, s^{\alpha}} \qquad \alpha \in \mathbb{R} \tag{1}$$

where $1/\tau_c^{-\alpha} = \omega_c$ is the gain crossover frequency, that is, $|L(\omega_c)| = 1$. The parameter α is the slope of the magnitude curve, on log–log scale, and may assume integer as well as non-integer values. In fact, the transfer function $L(s)$ is a fractional-order differentiator when $\alpha > 0$ and a fractional-order integrator for $\alpha < 0$. The Bode diagrams of $L(s)$, are very simple. The amplitude curve is a straight line of constant slope -20α dB/dec, and the phase curve is a horizontal line at $-\alpha\pi/2$ rad.

Let us now consider the unity feedback system represented in Fig. 1 with Bode's ideal transfer function $L(s)$ inserted in the forward path. This choice of $L(s)$ gives a closed-loop system with the desirable property of being insensitive to gain changes. If the gain changes, the crossover frequency ω_c will vary but the phase margin of the system remains equal to $\pi(1-\alpha/2)$ rad, independently of the value of the gain.

The closed-loop system of Fig. 1 is given by

$$G_{cl}(s) = \frac{C(s)G(s)}{1+C(s)G(s)} \tag{2}$$

and the desired closed-loop transfer function is given by

$$F(s) = \frac{L(s)}{1+L(s)} = \frac{1}{1+\tau_c\, s^{\alpha}} \qquad \alpha \in \mathbb{R}^+ \tag{3}$$

is used as a reference model for tuning the controller $C(s)$. It exhibits important properties such as infinite gain margin and constant phase margin (dependent only on α). Thus, this closed loop system is robust to process gain variations and the step response exhibits iso-damping property. As for this reference system, the order α and the time constant τ_c determine the overshoot (dependent on α) and the settling time (dependent on τ_c), respectively [25].

Then, for the case when we have the open loop transfer function ($G_{OL}(s) = G(s)C(s)$) close to $L(s)$, the closed loop response of this system will also behave like the closed loop response of the reference system $F(s)$ giving us the important properties of the reference system. Thus, to obtain the important properties of the closed loop system, the controller $C(s)$ is carried out so that the open loop ($G_{OL}(s) = G(s)C(s)$) is close to the open loop reference model $L(s)$. This is the CRONE principle [3,4] that all the proposed methods of fractional controllers tuning in frequency domain try to obtain.

2.2. Internal model control (IMC)

A more comprehensive model-based design method, internal model control (IMC), was developed by Morari and coworkers [26–28]. The IMC method, as the direct synthesis method usually used in the conventional feedback control, is based on assumed process models and leads to analytical expressions for the controller settings. These two design methods are closely related and produce identical controllers if the design parameters are specified in a consistent manner, for several models. However, the IMC approach has the advantage that it allows model uncertainty and tradeoffs between performance and robustness to be considered in a more systematic way.

The IMC paradigm is based on the simplified block diagram as shown in Fig. 2. A process model $G_m(s)$ and the controller output u are used to calculate the model response y_m. The model response is subtracted from the plant response y, and the difference $y-y_m$, is used as the input signal to the IMC controller $C_{IMC}(s)$. In general, $y \neq y_m$ due to modeling errors ($G_m(s) \neq G(s)$) and unknown disturbances $d \neq 0$ that are not accounted for in the model.

The block diagram for the conventional feedback control is given in Fig. 3. It can be shown that the two block diagrams are identical if controllers $C(s)$ and $C_{IMC}(s)$ satisfy the relation:

$$C(s) = \frac{C_{IMC}(s)}{1-C_{IMC}(s)G_m(s)} \tag{4}$$

Thus, any IMC controller $C_{IMC}(s)$ is equivalent to a standard feedback controller $C(s)$, and vice versa. The following closed loop

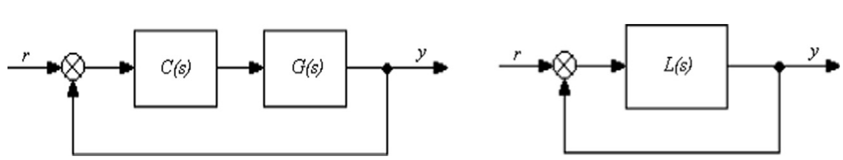

Fig. 1. Fractional-order control system with Bode's ideal transfer function.

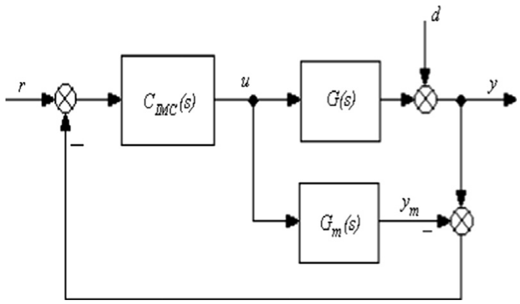

Fig. 2. Internal model control structure.

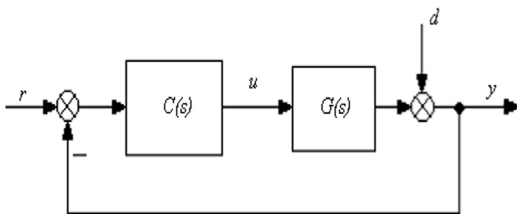

Fig. 3. Conventional feedback control.

relation for IMC can be driven from Fig. 3 taking into account Eq. (3).

$$y = \frac{C_{IMC}\, G}{1 + C_{IMC}(G - G_m)}\, r + \frac{1 - C_{IMC}\, G_m}{1 + C_{IMC}(G - G_m)}\, d \tag{5}$$

For the special case of a perfect model, $G_m(s) = G(s)$, Eq. (5) reduces to

$$y = C_{IMC}\, G\, r + (1 - C_{IMC}\, G_m)\, d \tag{6}$$

The IMC controller is designed in two steps [26]:

- *Step* 1: The process model is factored as

$$G_m(s) = G_m^+(s)\, G_m^-(s) \tag{7}$$

  where $G_m^+(s)$ contains any time delays and right-half plane zeros. $G_m^+(s)$ must have a steady-state gain equal to one.
- *Step* 2: The controller is specified as

$$C_{IMC}(s) = \frac{1}{G_m^-(s)} f(s) \tag{8}$$

  where $f(s)$ is a low pass filter with a steady-state gain of one. It typically has the form [6]:

$$f(s) = \frac{1}{(1 + \tau_c\, s)^r} \tag{9}$$

  In analogy with the direct synthesis method, τ_c is the desired closed loop time constant. Parameter r is a positive integer chosen so that the controller $C(s)$ is realizable. The usual choice is $r = 1$.

2.3. Design procedure

In this section, it is intended to propose some general principles dealing with FOPID controllers in order to justify their fractional structure and to propose some elementary design techniques satisfying robustness objectives represented by the CRONE principle. The main characteristic of our approach is the importance given to a closed loop reference model, including robustness and dynamical performances. The conventional feedback control shown in Fig. 3 is considered here where the plant transfer function $G(s)$ is integer. The proposed design technique is a generalization of PID tuning methods, based on the equivalence between IMC and conventional feedback. The main advantage of the IMC based controller design is the stability of the closed loop system. Indeed, the classic feedback structure and the IMC structure are entirely equivalent and the controllers $C_{IMC}(s)$ and $C(s)$ are related through Eq. (4). So, the IMC structure being internally stable, i.e., both the open loop plant $G(s)$ and the IMC controller $C_{IMC}(s)$ are stable, then the equivalent classic feedback structure is stable [26,28].

The details of the controller design for the proposed method is summarized in what follows.

Let $G_m(s)$ the model of an LTI integer order system.

Step 1 According to the IMC controller design, $G_m(s)$ must be factorized as

$$G_m(s) = G_m^+(s)\, G_m^-(s) \tag{10}$$

$G_m^-(s)$ is the nonsingular part of $G_m(s)$ and $G_m^+(s)$ is the singular part. ($G_m^+(s)$ contains the time delay and RHP-zeros of $G_m(s)$, its steady-state gain must be equal to one. Thus, the steady-state gain of $G_m(s)$ will remain in $G_m^-(s)$ which be used to design the IMC controller).

Step 2 The fractional property of the controller is introduced by the fractional reference model $f(s)$. To obtain the iso-damping property described in Section 2.1, $f(s)$ is given by

$$f(s) = \frac{1}{1 + \tau_c\, s^{\alpha+1}} \quad 0 < \alpha < 1 \tag{11}$$

The time constant τ_c and the non integer α are chosen to impose the phase margin φ_m and the crossover frequency ω_c of the closed-loop.

$$\alpha = \frac{\pi - \varphi_m}{\pi/2} - 1 \quad \textit{and} \quad \tau_c = \frac{1}{\omega_c^{\alpha+1}} \tag{12}$$

Step 3 The IMC Controller is calculated by

$$C_{IMC}(s) = \frac{1}{G_m^-(s)} f(s) \tag{13}$$

Step 4 The standard feedback controller $C(s)$ is the then

$$C(s) = \frac{C_{IMC}(s)}{1 - C_{IMC}(s) G_m(s)} \tag{14}$$

Step 5 As we show in Section 3, the controller $C(s)$ can be put in the form of an integer PID structure cascaded with a fractional filter $H(s)$

$$C(s) = H(s).K_p\left(1 + \frac{1}{\tau_i\, s} + \tau_d\, s\right) \tag{15}$$

3. IMC-PID-fractional-filter controllers design

In this section, we present the details of the method developed in this paper. The objective of the design is to control an integer open loop process with closed-loop specifications having fractional characteristics as given in Eq. (11). The idea is to have the controller with an integer PID structure as the open-loop system is integer, cascaded with a fractional filter to meet closed-loop fractional specifications. The general structure of the controller is given by

$$C(s) = \underbrace{H(s)}_{\textit{fractional filter}}\ \underbrace{K_p\left(1 + \frac{1}{\tau_i\, s} + \tau_d\, s\right)}_{\textit{Integer PID Controller}} \tag{16}$$

PID parameters are K_p is the gain, τ_i is the integral time constant, τ_d is the derivative time constant, and $H(s)$ is the fractional part of the controller.

We present in what follows how to get the form of $C(s)$ for four models often encountered in the literature. Table 2 in the appendix, gives the filter $H(s)$ and the parameters K_p, τ_i and τ_d of the integer PID for more other models.

Let us consider the delay-free integer system

$$G_m(s)=\frac{N(s)}{D(s)}. \tag{17}$$

We assume that neither $N(s)$ or $D(s)$ does have roots in the right half-plane of the complex plane. In addition, $G_m(s)$ is assumed to be strictly proper. In this case, using Eq. (8), the IMC controller is given by

$$C_{IMC}(s)=\frac{D(s)}{N(s)}\frac{1}{1+\tau_c\, s^{\alpha+1}} \tag{18}$$

and the conventional controller $C(s)$ is then deduced, it is given by

$$C(s)=\frac{D(s)}{N(s)\tau_c\, s^{\alpha+1}}=\frac{1}{s^\alpha}\frac{D(s)}{\tau_c\, s\, N(s)} \tag{19}$$

Note that $C(s)$ is composed of two transfer functions: the fractional integrator $1/s^\alpha$ (which characterizes the fractional aspect of the controller) and the integer order $D(s)/\tau_c\, s\, N(s)$ which can be factorized in the usual integer PID controller form. In what follows, four examples are studied. In each case, we show that $C(s)$ can be put in the general form given by Eq. (16).

3.1. Delay-free all-pole model

Assume that the plant is described by the integer second order model

$$G_m(s)=\frac{K}{T\, s^2+2\xi T\, s+1} \tag{20}$$

the closed loop reference model is that given by Eq. (11). The IMC controller is then

$$C_{IMC}(s)=\frac{T\, s^2+2\xi T\, s+1}{K(1+\tau_c\, s^{\alpha+1})} \tag{21}$$

The equivalent feedback controller is

$$C(s)=\frac{1}{s^\alpha}\frac{T\, s^2+2\xi T\, s+1}{K\, \tau_c\, s} \tag{22}$$

which can be written as

$$C(s)=\frac{1}{s^\alpha}\frac{2\, T\, \xi}{K\, \tau_c}\left(1+\frac{1}{2\, T\, \xi\, s}+\frac{1}{2\, \xi}s\right) \tag{23}$$

$C(s)$ is thus a classical integer PID controller cascaded with the fractional integrator $1/s^\alpha$.

3.2. Non-minimum phase model

Let us consider a plant described by the delay-free non minimal phase model

$$G_m(s)=\frac{K(1-Bs)}{(1+T_1 s)(1+T_2 s)} \quad B>0 \tag{24}$$

according to Eq. (7), $G_m(s)$ should be factored as

$$G_m(s)=\frac{K}{(1+T_1 s)(1+T_2 s)}\,(1-Bs) \tag{25}$$

the reference model is, in this case, also given by Eq. (9). So, according to Eq. (8), The IMC controller is

$$C_{IMC}(s)=\frac{(1+T_1 s)(1+T_2 s)}{K(1+\tau_c\, s^{\alpha+1})} \tag{26}$$

The equivalent feedback controller is then given by

$$C(s)=\frac{(1+T_1 s)(1+T_2 s)}{K(\tau_c\, s^{\alpha+1}+Bs)}=\frac{1+(T_1+T_2)s+T_1T_2s^2}{KBs\left(1+\frac{\tau_c}{B}\, s^\alpha\right)} \tag{27}$$

which can be written as

$$C(s)=\frac{1}{1+\frac{\tau_c}{B}\, s^\alpha}\frac{T_1+T_2}{KB}\left(1+\frac{1}{(T_1+T_2)s}+\frac{T_1+T_2}{(T_1+T_2)}s\right) \tag{28}$$

In this case also, $C(s)$ is an integer PID controller cascaded with the fractional filter $1/(1+\tau_c/B)\, s^\alpha$.

3.3. Integrating first-order model

Assume that the plant is described by

$$G_m(s)=\frac{K}{s(1+T\, s)}. \tag{29}$$

According to Eq. (8), the IMC controller is

$$C_{IMC}(s)=\frac{s(1+Ts)}{K(1+\tau_c\, s^{\alpha+1})} \tag{30}$$

The corresponding feedback controller is given by

$$C(s)=\frac{s(1+Ts)}{K(1+\tau_c\, s^{\alpha+1})} \tag{31}$$

with is written as

$$C(s)=\frac{1}{s^\alpha}\frac{1}{K_,\tau_c}(1+T\, s) \tag{32}$$

$C(s)$ is a classical PD controller cascaded with the fractional integrator $1/s^\alpha$.

3.4. First-order plus time delay model

In this last case, let us consider the most encountered model in the industry, represented by the transfer function, for which (θ/T) is small

$$G_m(s)=\frac{K\, e^{-\theta s}}{1+Ts} \tag{33}$$

3.4.1. First-order Padé approximation of the $e^{-\theta s}$ term

The time delay term is approximated by a first-order Padé approximation:

$$e^{-\theta s}=\frac{1-\frac{\theta}{2}s}{1+\frac{\theta}{2}s} \tag{34}$$

Substituting the time delay approximation in $G_m(s)$ and using Eq. (8), the IMC controller is

$$C_{IMC}(s)=\frac{(1+Ts)(1+\frac{\theta}{2}s)}{K(1+\tau_c\, s^{\alpha+1})} \tag{35}$$

Thus, the corresponding feedback controller is

$$C(s)=\frac{(1+Ts)\left(1+\frac{\theta}{2}s\right)}{K\left(\tau_c s^{\alpha+1}+\frac{\theta}{2}s\right)}=\frac{1+\frac{2T+\theta}{2}s+\frac{T\theta}{2}s^2}{\frac{KB}{2}\, s\left(1+\frac{2\tau_c}{\theta}\, s^\alpha\right)} \tag{36}$$

which can be written as

$$C(s)=\frac{1}{1+\frac{2\tau_c}{\theta}s^\alpha}\frac{2T+\theta}{K\theta}\left(1+\frac{1}{\frac{2T+\theta}{2}\, s}+\frac{T\theta}{2T+\theta}s\right) \tag{37}$$

Once again, $C(s)$ is an integer PID controller cascaded with the fractional filter $1/(1+(\sqrt{i}2T/\theta)s^\alpha)$.

3.4.2. First order Taylor expansion of the $e^{-\theta s}$ term

In this case, the time delay term is approximated by

$$e^{-\theta s} = 1 - \theta s \tag{38}$$

The step responses of the first order system with delay and its approximation are similar for small θ/T. Substituting the time delay approximation in $G_m(s)$ and using Eq. (8), the IMC controller is

$$C_{IMC}(s) = \frac{(1+Ts)}{K(1+\tau_c\, s^{\alpha+1})} \tag{39}$$

Thus, the corresponding feedback controller is

$$C(s) = \frac{(1+Ts)}{K(\tau_c\, s^{\alpha+1}+\theta s)} = \frac{1+Ts}{K\theta s\left(1+\frac{\tau_c}{\theta}s^{\alpha}\right)} \tag{40}$$

which can be written as

$$C(s) = \frac{1}{1+\frac{\tau_c}{\theta}s^{\alpha}}\,\frac{T}{K\theta}\left(1+\frac{1}{Ts}\right) \tag{41}$$

$C(s)$ is then a usual PI controller cascaded with the fractional filter $1/(1+(\tau_c/\theta)s^{\alpha})$.

As we have just seen, one of the main advantages of the proposed method is that it has no restriction on the class of process models. Tuning rules by the IMC method for other more complicated process models such as integrating and inverse processes with time delays are also listed in Tables 2 and 3 in the Appendix.

4. Numerical examples

In this section, the IMC-PID-fractional-filter controller design is applied to typical models encountered in the industry. Simulation studies were carried out on two integer order processes found in the literature. The first one is a first order plus time delay system taken from [14]. The second example is a second order delay free system reported in [29].

All time-responses involving fractional derivatives and integrals are obtained with simulation making use of Oustaloup's approximation in appropriate frequency range. The simulation scheme is shown in Fig. 4, where $G(s)$ is the plant, $G_d(s)$ is the disturbance transfer function and $C(s)$ is the controller. r is a unit step applied at $t=0$ and d is a step disturbance applied in steady state of the output. n is white noise added to the output signal.

4.1. Example 1

The first example is an experimental platform which consist of a low pressure flowing water circuit which is bench mounted and completely self contained [14]. The liquid level system is modeled by a first-order transfer function given by

$$G(s) = \frac{k}{Ts+1}e^{-Ls} \tag{42}$$

characterized by the gain $k=3.13$, the time constant $T=433.33$ s and a time delay $L=50$ s.

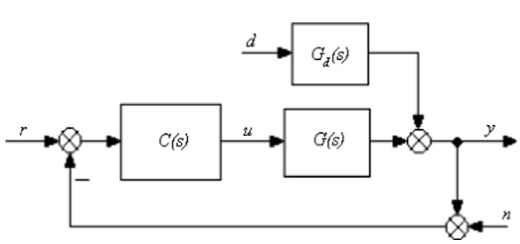

Fig. 4. Simulation scheme.

The tuning method of the fractional order $PI^{\lambda}D^{\mu}$–controller proposed in [14] is made so that the closed-loop system fulfills five specifications regarding to plant uncertainties (especially gain variation) load disturbances and high frequency noise. The specifications are

- gain crossover frequency: $\omega_c = 0.008$ rad/s;
- phase margin: $\varphi_m = 60\circ$;
- robustness to variations in the gain: $\left(\frac{d(C(j\omega)G(j\omega))}{d\omega}\right)_{\omega=\omega_c} = 0$;
- sensitivity function: $|S(j\omega)|_{dB} \le -20$ dB, $\forall \omega \le 0.001$ rad/s;
- noise rejection: $|T(j\omega)|_{dB} \le -20$ dB, $\forall \omega \ge 10$ rad/s.

Because of the complexity of this set of nonlinear equations, the FMINCON function of the optimization toolbox of Matlab has been used to reach out the best solution. The first specification is taken as the main function to minimize, and the rest of specifications are taken as constraints for the minimization (see [14] for more detail). Applying this optimization method, the fractional order $PI^{\lambda}D^{\mu}$–controller obtained by Monje et al. is

$$C(s) = 0.6152 + \frac{0.010}{s^{0.8968}} + 4.3867\, s^{0.4773}. \tag{43}$$

For this same example, the controller settings are calculated using our proposed method and are summarized in Table 1. For proper selection of the tuning parameters α and τ_c, gain crossover frequency, $\omega_c = 0.008$ rad/s and phase margin, $\varphi_m = 60^\circ$ are taken. We found $\alpha = 0.1111$ and $\tau_c = 136.22$ s. Applying the proposed method, the PI-fractional-filter controller obtained is given by

$$C(s) = \frac{2.7689}{1+2.7444\, s^{0.1111}}\left(1+\frac{1}{433.33\, s}\right) \tag{44}$$

The fractional integral and derivative have been implemented by the Oustaloup continuous approximation choosing a frequency band from 0.001 to 10 rad/s using 8 cells by decade. The Bode plots of the open-loop system are shown in Fig. 5. This figure shows that the specifications of gain crossover frequency and phase margin are met in both cases.

Fig. 6 shows the dynamic response characteristics of the closed-loop system with a unit step change in the setpoint $r(t)$ at $t=0$ s and a negative step disturbance $d(t)$ of magnitude 0.1 at $t=1500$ s. The disturbance transfer function is arbitrary considered as $G_d(s) = 1/(1+100\, s)$. As can be observed, the proposed method provides better performance for both set point tracking and disturbance rejection. Table 1 summarizes the characteristics of the Bode plot of the open-loop and the step response of the closed-loop system. From this table, it can be observed that the overshoot is bigger with the method proposed by Monje et al. nevertheless, the step response is established more slowly with our method.

Fig. 7 shows the control law obtained with the proposed method and that of Monje et al. One can observe the advantage of the proposed method since the maximum value is 13.8 V with the method given by Monje et al. and only 1.19 V with the proposed method. To further analyze the robustness of the two methods, variations in the gain and the time constant of the plant have been considered. Figs. 8 and 9 show the results obtained respectively.

Table 1
Characteristics of Bode plot of the open-loop and the step response of the closed-loop.

	ω_c (rad/s)	φ_m (deg)	M_p (%)	t_s (2%)
Reference model	0.008	60	8.8	1330
Proposed method	0.0078	57.6	11.55	1330
Monje et al. method	0.008	59.4	13.35	752

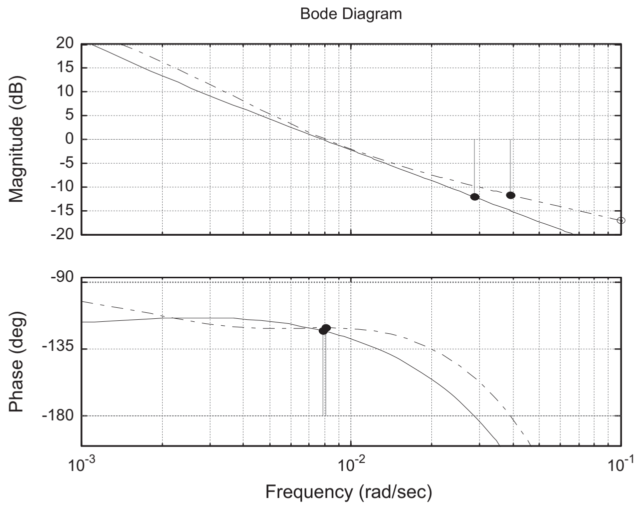

Fig. 5. Bode plot of the open-loop system: solid line – proposed method; dashed line – Monje et al. [14].

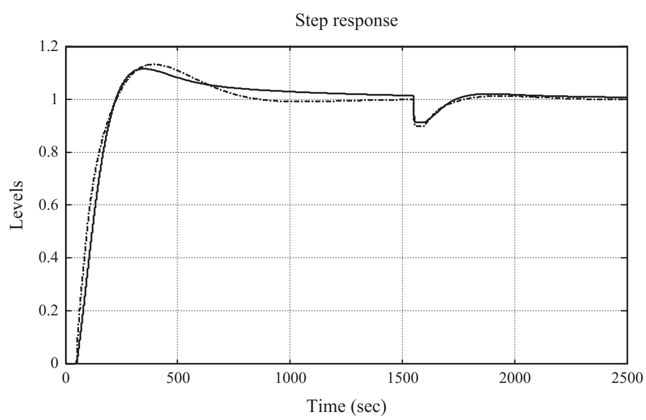

Fig. 6. Step responses the closed-loop system with disturbance: solid line – proposed method; dashed line – Monje et al. [14].

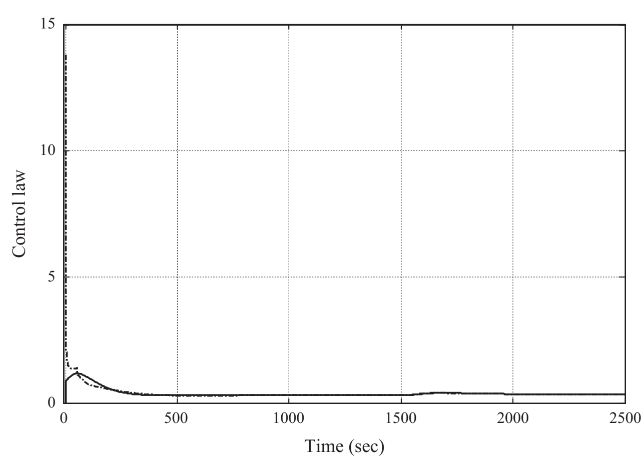

Fig. 7. Control law applied to the controlled system: solid line – proposed method; dashed line – Monje et al. [14].

Fig. 8 shows that the method proposed by Monje et al. is better because only a slight variation in the peak value of the output response is produced when the gain changes. Indeed, as shown in Fig. 5 with the method proposed by Monje et al., the phase of the open-loop system is forced to be flat at w_c and hence to be almost

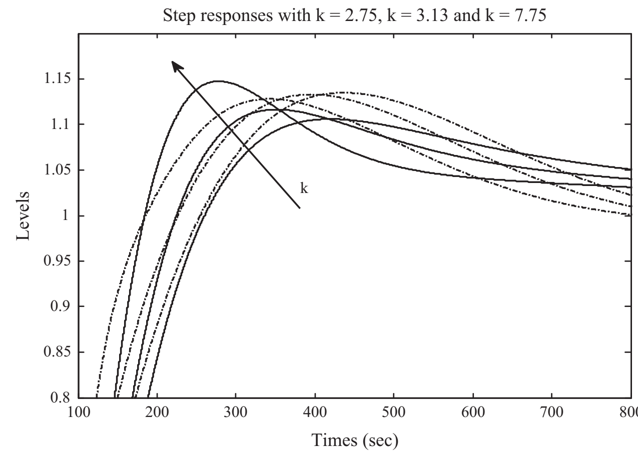

Fig. 8. Step responses with k variations: solid line – proposed method; dashed line – Monje et al. [14].

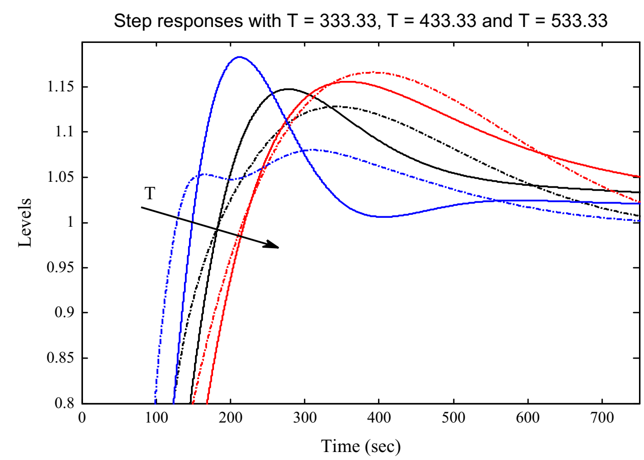

Fig. 9. Step responses with T variations: solid line – proposed method; dashed line – Monje et al. [14].

constant within an interval around w_c. This is not the case with our method. however, when the time constant changes, the proposed method is better.

Finally, to show the robustness of the two controllers with respect to measurement noise, a white noise sequence with zero mean, unit variance and a frequency equal to 100 Hz is added to the measured signal. The complementary sensitivity function is plotted in Fig. 10. This figure shows that the high frequency signals are filtered better with the proposed controller. Fig. 11 shows the impact of this feature on the quality of the output signal. It can be observed that the output signal is much noisy with the fractional order *PID* controller proposed by Monje et al.

4.2. Example 2

This example treats the fractional order controller in the angular velocity control of a servo system. The servo system includes the modules of DC motor with tacho-generator, inertia load, encoder and gearbox with output disk (see [29] for more details). For the identification experiment, a unit step input is applied to the servo system and the process output is acquired. The input–output data were transmitted to us by Barbosa.

To design the fractional controllers, Barbosa et al. used the method of Ziegler–Nichols based on the estimated first order plus

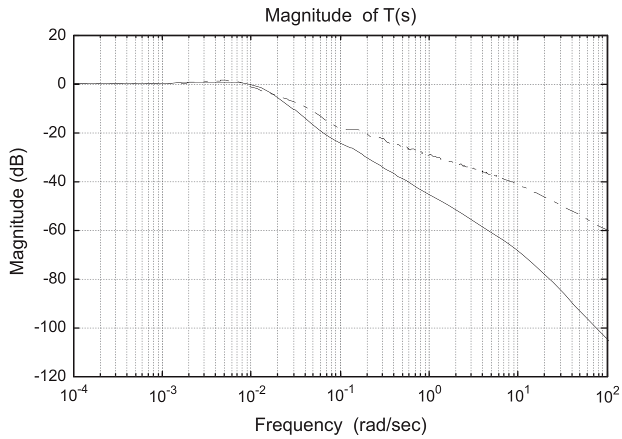

Fig. 10. Magnitude of the complementary sensitivity function: solid line – proposed method; dashed line – Monje et al. [14].

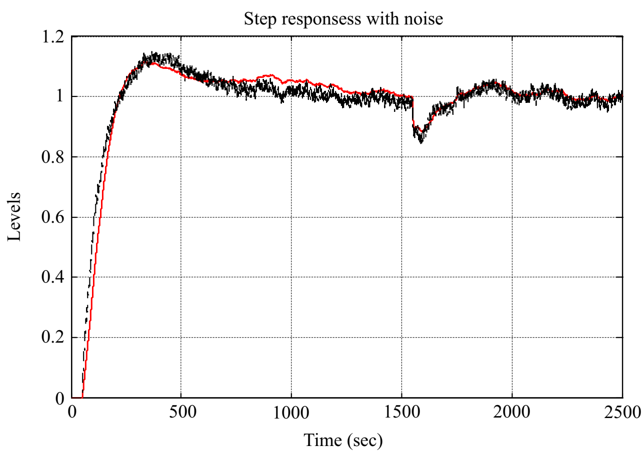

Fig. 11. Step responses of closed-loop system with noise: solid line – proposed method; dashed line – Monje et al. [14].

time delay model, given by

$$G(s)=\frac{187.2106}{1+1.1841\ s}e^{-0.1753\ s} \quad (45)$$

In our case, the controller design is based on the estimated second order delay free model, given by

$$G(s)=\frac{187.2106}{(1+0.74\ s)(1+0.3\ s)} \quad (46)$$

in Fig. 12, we show the experiment step response, the step responses simulation of the FOPTD model (45) and the second order model (46).

The experimental test bench being unavailable, the comparison between the controller proposed by Barbosa et al. and that proposed here will be realized on a more complex model estimated once again from the experimental data. This last is estimated using Levenberg–Marquardt algorithm [30].

The fractional controller proposed in [29] is a $PI^{\mu}D-$controller. The parameters of the controller are those of an integer *PID*-controller obtained from the Ziegler–Nichols rules. In [Section (6) 29], authors have studied the effect of the fractional order of a $PI^{\mu}D-$controller in the velocity control. Step responses of the angular velocity for several values of integrative order μ have been presented. To compare between the $PI^{\mu}D-$controller proposed by Barbosa et al. and the PID-fractional-order-filter controller (*PID-FOF*-controller) proposed here, we used the value $\mu=04$ which seems to give a good tradeoff between the overshoot

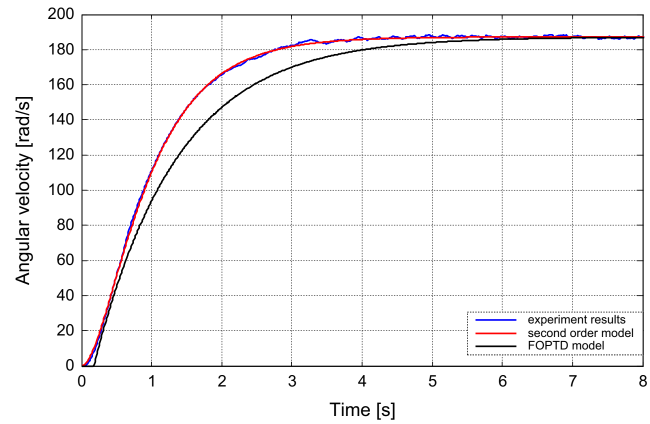

Fig. 12. Unit step response: blue: of servo system, red: second order model, and black: FOPTD model. (For interpretation of the references to color in this figure caption, the reader is referred to the web version of this paper.)

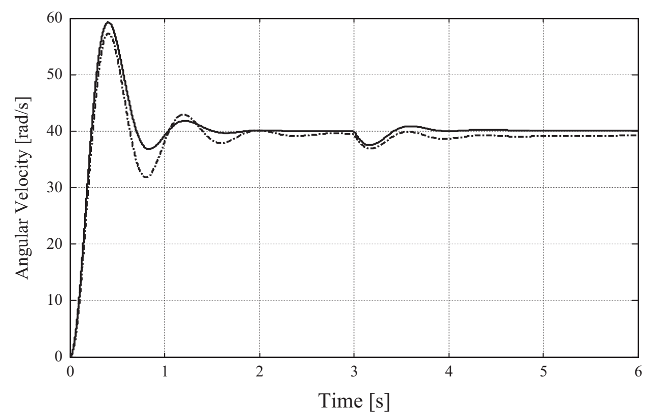

Fig. 13. Closed-loop step response: solid line – proposed method; dashed line – Barbosa et al. [29].

and the settling time. The $PI^{\mu}D-$controller proposed by Barbosa et al. is

$$C(s)=0.0433+\frac{0.1235}{s}+0.0038s \quad (47)$$

Though the damping is usually related with the phase margin, and the settling time is related with the gain crossover frequency, there are no analytical formulas that express these relations in the case of process (46) controlled by (47). To design the parameters of the *PID-FOF*-controller, we have plotted the step response of the closed-loop system and measured the value of the overshoot. We estimate the frequency specifications $\varphi_m=34\circ$. and $\omega_c=$ 8.16 rad/s that could approximately achieve the above temporal specifications for the given nominal model (46) controlled by (47). These values are then used to achieve the parameters values $\alpha=0.6222$ and $\tau_c=0.0332$ s, of the closed-loop reference model of Eq. (16). The open-loop model to be controlled being a two time constants model, using Table 2 given in the appendix, the *PID-FOF*-controller obtained is given by

$$C(s)=\frac{0.1674}{s^{0.6222}}\left(1+\frac{1}{1.04\ s}+0.2135s\right). \quad (48)$$

A magnitude 40 step setpoint input is added at $t=0$ and an inverse step load disturbance of magnitude 3 is added to the process output at $t=3$ s. The disturbance transfer function is $G_d(s)=1/(1+0.74s)$. Simulation results are shown in Fig. 13. Fig. 14 shows the Bode plot of the open-loop system. Fig. 14 shows the specifications of gain crossover frequency and phase margin

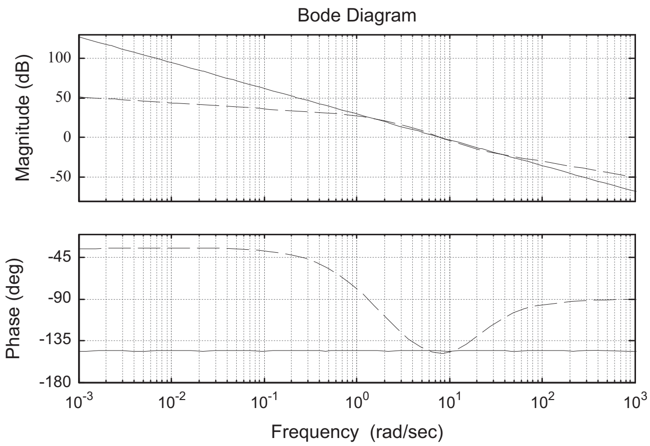

Fig. 14. Bode plots of the open-loop system: solid line – proposed method; dashed line – Barbosa et al. [29].

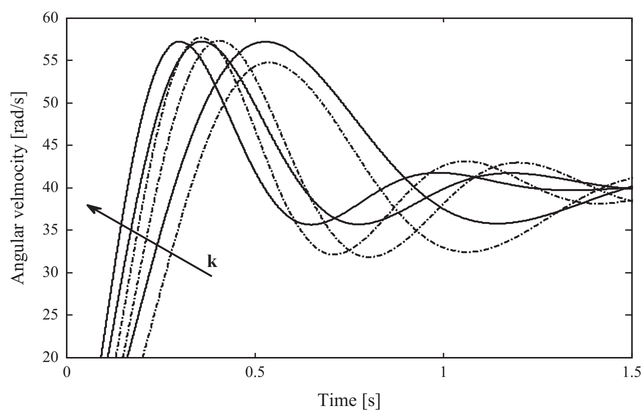

Fig. 15. Closed-loop step responses with gain variation: solid line – proposed method; dashed line – Barbosa et al. [29].

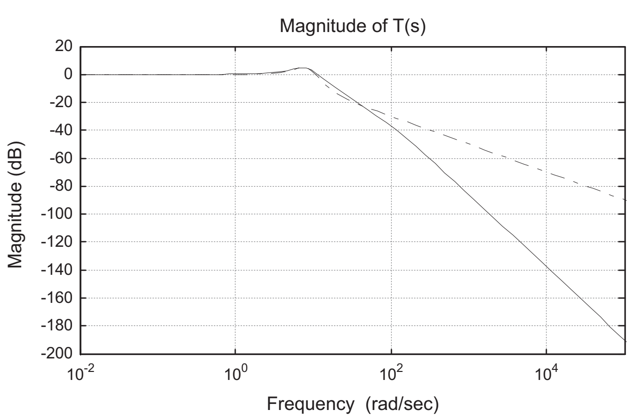

Fig. 16. Magnitude plots of the sensitivity function: solid line – proposed method; dashed line – Barbosa et al. [29].

are met in both cases. It can seen from Fig. 13 that both $PI^{\mu}D-$controller and *PID-FOF*-controller are effective. Nevertheless, it should be noted that the $PI^{\mu}D-$controller converge slowly to the target value. This is due to the fact that this controller have insufficient gain at low frequencies (see Fig. 14) contrary to the *PID-FOF*-controller.

In Fig. 15, applying the $PI^{\mu}D-$controller of Barbosa et al. (dashed line) and the proposed *PID-FOF*-controller (solid line), the output step responses are plotted with the open-loop gain variation from 125 to 250 ($\pm$34% variation from the nominal value

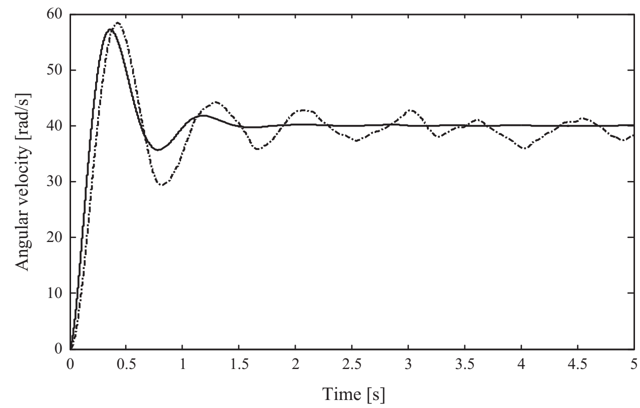

Fig. 17. Closed-loop step responses with noise: solid line – proposed method; dashed line – Barbosa et al. [29].

187.2106). From Fig. 15, it can be seen obviously that the overshoot of the *PID-FOF*-controller (solid line) remain constant under gain variations, i.e., the iso-damping property is exhibited.

To show the robustness of the two controllers with respect to measurement noise, a white noise sequence with magnitude 3, zero mean, unit variance and a frequency equal to 10 Khz is added to the measured signal. The complementary sensitivity function is plotted in Fig. 16. This figure shows that the high frequency signals are filtered better with the proposed controller. Fig. 17 shows the impact of this feature on the quality of the output signal. It can be observed that with the *PID-FOF*-controller (solid line), the step response have not change but with the $PI^{\mu}D-$controller, the output signal has changed (as compared to Fig. 13). So we can see that the *PID-FOF*-controller outperforms the $PI^{\mu}D-$controller.

5. Conclusion

The paper presented a simple analytical PID-fractional-filter controller design method based on the IMC paradigm for integer processes. The proposed PID-fractional-filter is composed of an integer order PID cascaded with a fractional filter. It can thus easily to be implemented on the modern control hardware. The fractional IMC/filter is more attractive than the integer one as it has the iso-damping robustness property as well as more degrees of freedom to meet other specifications. The proposed design method is also simple to apply and can be used for several models commonly encountered in industry as shown in Tables 2 and 3. Tow representative processes frequently used in many previous studies were considered in the simulation study. The simulation was conducted by tuning the controller parameters to obtain in the closed loop step response, a desired settling time (dependent on the time constant τ_c) and desired overshoot (dependent on the non integer order (α)). The proposed method has given improved results in both the setpoint tracking and disturbance rejection. Future works are underway to apply the proposed PID-fractional-filter controller design for large scale systems and long dead time systems.

Appendix A

See Tables 2 and 3.

Table 2
IMC-PID-fractional-filter for delay free processes.

$G_m(s)$	Fract. filter	K_p	τ_i	τ_d
$\frac{K}{1+T\,s}$	$\frac{1}{s^\alpha}$	$\frac{T}{K\,\tau_c}$	T	–
$\frac{K}{(1+T_1\,s)(1+T_2\,s)}$	$\frac{1}{s^\alpha}$	$\frac{T_1+T_2}{K\,\tau_c}$	T_1+T_2	$\frac{T_1T_2}{T_1+T_2}$
$\frac{K}{T^2s^2+2\xi Ts+1}$	$\frac{1}{s^\alpha}$	$\frac{2\xi T}{K\,\tau_c}$	$2\xi T$	$\frac{1}{2\xi}$
$\frac{K}{s}$	$\frac{1}{s^\alpha}$	$\frac{1}{K\,\tau_c}$	–	–
$\frac{K}{s(1+T\,s)}$	$\frac{1}{s^\alpha}$	$\frac{1}{K\,\tau_c}$	–	T
$\frac{K(1-Bs)}{T^2s^2+2\xi Ts+1}$	$\frac{1}{1+\frac{\tau_c}{B}s^\alpha}$	$\frac{2\xi T}{K\,B}$	$2\xi T$	$\frac{T}{2\xi}$
$\frac{K(1-Bs)}{(1+T_1\,s)(1+T_2\,s)}$	$\frac{1}{1+\frac{\tau_c}{B}s^\alpha}$	$\frac{T_1+T_2}{K\,B}$	T_1+T_2	$\frac{T_1T_2}{T_1+T_2}$

Table 3
IMC-PID-Fractional-filter for processes with delay (first line, first order Taylor expansion, second line, first order Padé approximation).

$G_m(s)$	Fract. filter	K_p	τ_i	τ_d
$\frac{Ke^{-\theta s}}{1+Ts}$	$\frac{1}{1+\frac{\tau_c}{\theta}s^\alpha}$ $\frac{1}{1+\frac{2\tau_c}{\theta}s^\alpha}$	$\frac{T}{K\theta}$ $\frac{2T+\theta}{K\theta}$	T $\frac{2T+\theta}{2}$	– $\frac{T\theta}{2T+\theta}$
$\frac{Ke^{-\theta s}}{s}$	$\frac{1}{1+\frac{\tau_c}{\theta}s^\alpha}$ $\frac{1}{1+\frac{2\tau_c}{\theta}s^\alpha}$	$\frac{1}{K\theta}$ $\frac{2}{K\theta}$	– –	– $\frac{\theta}{2}$
$\frac{Ke^{-\theta s}}{s(1+Ts)}$	$\frac{1}{1+\frac{\tau_c}{\theta}s^\alpha}$ $\frac{1}{1+\frac{2\tau_c}{\theta}s^\alpha}$	$\frac{1}{K\theta}$ $\frac{2}{K\theta}\ (1+Ts)\ (1+\frac{\theta}{2}\ s)$	–	T
$\frac{Ke^{-\theta s}}{T^2s^2+2\xi Ts+1}$	$\frac{1}{1+\frac{\tau_c}{\theta}s^\alpha}$ $\frac{1}{1+\frac{2\tau_c}{\theta}s^\alpha}$	$\frac{2\xi T}{K\theta}$ $\frac{4\xi T}{K\theta}$	$2\xi T$ $2\xi T$	$\frac{T}{2\xi}$ $\frac{T}{2\xi}$
$\frac{Ke^{-\theta s}}{(1+T_1s)(1+T_2s)}$	$\frac{1}{1+\frac{\tau_c}{\theta}s^\alpha}$ $\frac{1}{1+\frac{2\tau_c}{\theta}s^\alpha}$	$\frac{T_1+T_2}{K\theta}$ $\frac{2(T_1+T_2)}{K\theta}$	T_1+T_2 T_1+T_2	$\frac{T_1T_2}{T_1+T_2}$ $\frac{T_1T_2}{T_1+T_2}$
$\frac{K(1+T_3s)e^{-\theta s}}{(1+T_1s)(1+T_2s)}$	$\frac{1}{1+T_3s}\frac{1}{1+\frac{\tau_c}{\theta}s^\alpha}$ $\frac{1+\frac{\theta}{2}s}{1+T_3s}\frac{1}{1+\frac{2\tau_c}{\theta}s^\alpha}$	$\frac{T_1+T_2}{K\theta}$ $\frac{2(T_1+T_2)}{K\theta}$	T_1+T_2 T_1+T_2	$\frac{T_1T_2}{T_1+T_2}$ $\frac{T_1T_2}{T_1+T_2}$
$\frac{K(1-Bs)e^{-\theta s}}{1+Ts}$	$\frac{1}{\tau_cs^\alpha-\theta Bs+\theta+B}$ $\frac{1}{\tau_cs^\alpha-\frac{\theta B}{2}s+\frac{\theta}{2}+B}$	$\frac{T}{K}$ $\frac{2\,T+\theta}{2\,K}$	T $T+\frac{\theta}{2}$	– $\frac{T\theta}{2T+\theta}$
$\frac{K(1-Bs)e^{-\theta s}}{T^2s^2+2\xi Ts+1}$	$\frac{1}{\tau_cs^\alpha-\theta Bs+\theta+B}$ $\frac{1+\frac{\theta}{2}s}{\tau_cs^\alpha-\frac{\theta B}{2}s+\frac{\theta}{2}+B}$	$\frac{2\xi T}{K}$ $\frac{2\xi T}{K}$	$2\xi T$ $2\xi T$	$\frac{T}{2\xi}$ $\frac{T}{2\xi}$
$\frac{K(1-Bs)e^{-\theta s}}{s(1+Ts)}$	$\frac{1}{\tau_cs^\alpha-\theta Bs+\theta+B}$ $\frac{1}{\tau_cs^\alpha-\theta Bs+\theta+B}$	$\frac{1}{K}$ $\frac{T}{K}$	– T	T –

Table 3 (*continued*)

$G_m(s)$	Fract. filter	K_p	τ_i	τ_d
	$\frac{1}{\tau_cs^\alpha-\theta Bs+\theta+B}$ $\frac{1}{\tau_cs^\alpha-\theta Bs+\theta+B}$	$\frac{1}{K}\ (1+Ts)\ (1+\frac{\theta}{2}\ s)$ $\frac{T}{K}$	 T	 –

References

[1] Astrom KJ, Hagglund T. PID controllers: theory, design and tuning. Research Triangle Park, NC: Instrument Society of America; 1995.
[2] Silva GJ, Datta A, Bhattacharyya SP. PID controllers for time-delay systems. Boston: Birkhäuser; 2005.
[3] Yeroglu C, Tan N. Classical controller design techniques for fractional order case. ISA Trans 2011;50:1461–72.
[4] Ozbay H, Bonnet C, Fioravanti AR. PID controller design for fractional-order systems with time delays. Syst Control Lett 2012;61:18–23.
[5] Narang A, Shah SL, Chen T. Tuning of fractional PI controllers for fractional order system models with and without time delays. In: Proceedings of 2010 American control conference. Baltimore, Maryland, USA; June 30–July 02, 2010.
[6] Luo Y, Chen YQ, Wang CY, Pi YG. Tuning fractional order proportional integral controllers for fractional orders systems. In: Proceedings of control and decision conference, 2009. CCDC'09. Chinese; June 17–19, 2009. p. 307–12.
[7] Poblubny I. Fractional-order system and $PI^\lambda D^\mu$ controllers. IEEE Trans Autom Control 1999;44(1):208–14.
[8] Vinagre BM, Podlubny I, Dorcak L, Feliu V. On fractional PID controllers: a frequency domain approach. In: Proceeding of IFAC workshop on digital control: past, present and future of PID control, April 5–7, Terrasa, Spain; 2000. p. 53–8.
[9] Monje CA, Vinagre BM, Chen YQ, Feliu V, Lanusse P, Sabatier J. Proposals for fractional $PI^\lambda D^\mu$ tuning. In: Proceedings of FDA'10, the 1st IFAC workshop fractional differentiation and its applications, July 19–21, Bordeaux, France; 2004.
[10] Valerio D, Da-Costa JS. Tuning of fractional PID controllers with Ziegler–Nichols-type rules. Signal Process. 2006;86:2771–84.
[11] Mansouri R, Djennoune S, Bettayeb M. Fractional I–P pole placement controller design: application to permanent magnet synchronous motor control. Int J Model Identif Control 2008;4(2):176–85.
[12] Mansouri R, Bettayeb M, Djennoune S. Non integer order I–P pole placement controller design: application to induction motor control. Int Rev Electr Eng 2007;2(5):695–703.
[13] Das S, Saha S, Das S, Gupta A. On the selection of tuning methodology of FOPID controllers for the control of higher processes. ISA Trans 2011;50:376–88.
[14] Monje CA, Vinagre BM, Feliu V, Chen YQ. Tuning and auto-tuning of fractional order controllers for industry applications. Control Eng Pract 2008;16:798–812.
[15] Jesus IS, Machado JAT. Fractional control of heat diffusion systems. Nonlinear Dyn 2008;54:263–82.
[16] Domingues J, Valerio D, Da Costa JS. Rule-based fractional control of irrigation canal. In: Proceedings of the 35th annual conference of IEEE industrial electronics. (IECON'09), November 3–5, Porto Portugal; 2009.
[17] Zamani M, Ghartemani MK, Sadati N, Parniani M. Design of a fractional order PID controller for an AVR using particle swarm optimization. Control Eng Pract 2009;17:1380–7.
[18] Maamri N, Trigeassou J-C, Tenoutit M. On fractional PI and PID controllers. In: Proceedings of FDA'10, the 4th IFAC workshop fractional differentiation and its applications, October 18–20, Badajoz, Spain; 2010.
[19] Dazi L, Weiguang F, Qibing J, Tianwei T. An IMC-$PI^\lambda D^\mu$ controller design for fractional calculus system. In: Proceeding of the 29th Chinese control conference, July 29–31, Beijing, China; 2010.
[20] Vinoprada T, Sivakumaran N, Narayanan S. IMC based fractional order PID controller. In: IEEE International conference on industrial technology, March 14–16, Auburn, AL, USA; 2011.
[21] Tavakoli-Kakhki M, Haeri M. Fractional order model reduction approach based on retention of the dominant dynamics: application in IMC based tuning of FOPI and FOPID controllers. ISA Trans 2011;50:432–42.
[22] Oustaloup A. La commande CRONE. Paris: Hermés Edition; 1991.
[23] Oustaloup A, Mathieu B. La commande CRONE du scalaire au multivariable. Hermés Editeur, Paris; 1999.
[24] Bode HW. Network analysis and feedback amplifier design. New Tork: Van Nostrand; 1945.
[25] Barbosa RS, Machado JAT, Ferreira IM. Tuning of PID controllers based on Bode's ideal transfer function. Nonlinear Dyn 2004;38:305–21.
[26] Morari M, Zafiriou E. Robust process control. Englewood Cliffs: Prentice-Hall; 1991.
[27] Rivera DE, Morari M, Skogestad S. Internal model control 4. PID controller design. Ind. Eng. Chem. Process Des. Dev. 1986;25:252–65.
[28] Garcia CE, Morari M. Internal model control I. A unifying review and some new results. Ind. Eng. Chem. Process Des. Dev. 1982;21:308–21.
[29] Barbosa RS, Machado JAT, Jesus IS. Effect of fractional orders in the velocity control of a servo system. Comput Math Appl 2010;59:1979–86.
[30] Djamah T, Mansouri R, Djennoune S, Bettayeb M. Optimal low order model identification of fractional dynamic systems. Applied Mathematics and Computation 206(2):543-54.